Characterization of Al-Zr, Al-Hf and Al-Ce-pillared vermiculites by X-ray photoelectron spectroscopy

Ana María Campos[1], Sonia Moreno[2], Rafael Alberto Molina[2,*]

[1]Departamento de Ciencias Básicas, Facultad de Ciencias Naturales e Ingeniería, Universidad de Bogotá Jorge Tadeo Lozano, Bogotá, D.C., Colombia
[2]Estado Sólido y Catálisis Ambiental, Departamento de Química, Facultad de Ciencias, Universidad Nacional de Colombia, Bogotá, D.C., Colombia

Abstract

X-ray photoelectron spectroscopy was used to establish the relative concentration and the chemical environment of modifying species in a series of vermiculites pillared with mixed precursors of Al-Zr, Al-Hf and Al-Ce. The binding energies observed provided evidence that zirconium and hafnium are most likely found as Zr-O(H)- and/or Zr-Si- and HfO_2, displaying a larger dispersion on the vermiculite surface compared with cerium species (Ce_2O_3), which are mainly found inside clay aggregates. On the one hand, the chemical analysis showed that with Al-Hf and Al-Zr solutions, the introduction of hafnium and zirconium was complete within the range of 0.5 - 2 mmol g^{-1} of clay, but the efficiency was reduced with larger quantities. On the other hand, the introduction of cerium in the Al-Ce solutions can be considered to be complete within the range assessed.

Key words: Pillared vermiculite, zirconium, hafnium, cerium, XPS.

Caracterización de vermiculitas pilarizadas con Al-Zr, Al-Hf y Al-Ce por espectroscopía de fotoelectrones emitidos por rayos-X

Resumen

Se utilizó la espectroscopia de fotoelectrones emitidos por rayos-X para establecer la concentración relativa y el ambiente químico de las especies introducidas en una serie de vermiculitas pilarizadas con precursores mixtos de Al-Zr, Al-Hf y Al-Ce. Las energías de enlace observadas evidenciaron que es más probable encontrar zirconio y hafnio como Zr-O(H) - o Zr-Si-y HfO_2, y que estos exhiben, además, una mayor dispersión en la superficie de la vermiculita en comparación con las especies de cerio (Ce_2O_3), las cuales se encuentran principalmente en el interior de las láminas de arcilla. Por un lado, el análisis químico mostró que con las soluciones de Al-Hf y Al-Zr, la introducción de hafnio y de zirconio era completa dentro del rango de 0,5 a 2 mmol g^{-1} de arcilla, pero que la eficacia se reducía con cantidades más grandes. Por otro lado, la introducción de cerio en las soluciones de Al-Ce pudo considerarse completa dentro del rango evaluado.

Palabras clave: vermiculita pilarizada, zirconio, hafnio, cerio, XPS.

Introduction

Research carried out in the past few years regarding the pillaring of clay minerals with high interlayer charge has special interest in the study of new processes that allow for the control of physical-chemical properties, with an emphasis on the development of the acidity in these materials (**Vicente, *et al.***, 2013; **del Rey-Pérez-Caballero & Poncelet**, 2000a; **del Rey-Pérez-Caballero & Poncelet**, 2000b; **del Rey-Pérez-Caballero, *et al.***, 2000c; **Jiménez, *et al.***, 2005; **Cristiano, *et al.***, 2005). A characteristic feature of these materials is their efficiency as catalysts in proton-catalyzed reactions, as they possess a large number of substitutions in the tetrahedral sheet (Si-OH-Al bonds) (**del Rey-Pérez-Caballero & Poncelet**, 2000; **del Rey-Pérez-Caballero & Poncelet**, 2000b; **del Rey-Pérez-Caballero, *et al.***, 2000; **Jiménez, *et al.***, 2005; **Cristiano, *et al.***, 2005; **Chimielarz, *et al.***, 2007; **Hernández, *et al.***, 2007; **Hernández, *et al.***, 2008; **Campos, *et al.***, 2007).

In this sense, vermiculite is an attractive clay, with a large number of these substitutions as well as a high thermal stability (**Suvorov & Skurikhin**, 2003; **Campos, *et al.***, 2008; **Purceno, *et al.***, 2012). In fact, the acidic properties expected from pillared vermiculites have been highlighted due to their great activity and selectivity in reactions such as octane (**del**

***Corresponding author:**
Rafael Alberto Molina, Molinaramolinag@unal.edu.co
Recibido: 23 de Julio de 2014
Aceptado: 10 de diciembre de 2014

Rey-Pérez-Rodríguez, *et al.*, 2000c), heptane (**Cristiano, *et al.***, 2005) and decane hydroconversion (**Campos, *et al.***, 2007; **Suvorov & Skurikhin**, 2003; **Campos, *et al.***, 2008; **Campos, *et al.***, 2008b).

The pillaring of mixed systems of metal cations has proven to be a very useful process to increase and enhance the acidic properties in vermiculites. Aluminum is usually employed as the main cation, as it is expected that two of its main characteristics, i.e., its thermal stability and total acidity, will be enhanced through the addition of small molar fractions of a second cation due to the increase in active sites in some types of mixed oxides (**Valášková, *et al.***, 2013; **Trombetta, *et al.***, 2000). The characteristics of cations that may cause an increase in acidity are based on some elementary aspects of their chemistry in aqueous solution (**Jolivet, *et al.***, 1994), which may result in an important increase of the acidity in the final oxide (**Tanabe, *et al.***, 1989). Through this approach, vermiculites pillared with aluminum (**del Rey-Pérez-Caballero & Poncelet**, 2000; **del Rey-Pérez-Caballero & Poncelet**, 2000b; **del Rey-Pérez-Caballero, *et al.***, 2000; **Jiménez, *et al.*,** 2005; **Cristiano, *et al.***, 2005; **Chimielarz, *et al.***, 2007; **Hernández, *et al.*,** 2007; **Hernández, *et al.***, 2008), with Al-Zr (**Cristiano, *et al.***, 2005; **Campos, *et al.***, 2008) and with Al-Ce (**Campos, *et al.***, 2007; **Campos, *et al.***, 2008) have been reported. The modifications carried out have evidenced that the addition of strong acid cations to the aluminum polymer solution significantly promotes the acidic properties of materials compared with the simple aluminum systems (**Cristiano, *et al.***, 2005; **Campos, *et al.***, 2008). However, the studies on the behavior of pillaring species in vermiculites do not provide details about the chemical state and the environment of these species either on the outer surface or between the layers of clay minerals.

In this sense, X-ray photoelectron spectroscopy (XPS) is an ideal characterization technique. Given that electrons originate from a depth between 1 and 10 nm (**Weckhuysen, *et al.***, 2000), XPS is appropriate to study structural ions on clay 2:1, even for species located in the interlayer region (**He, *et al.***, 2007; **Pandolfi, *et al.***, 2008). In fact, the analysis on the clay surface may be extended to the structural analysis because of the thickness of the layers comprising these solids (**Gier & Jhons**, 2000). This extension has been confirmed by several studies regarding the depth of analysis on these materials (**Cool, *et al.***, 1997; **Jhons & Gier**, 2001), and results have shown a good correlation with elemental chemical analysis. However, differences approaching 10% in the relative concentration of the ions making up the layers have also been reported with respect to mass content, while the difference in the relative concentration of interlayer ions oscillated between 20 and 30% (**González, *et al.***, 1988). These differences have been associated with XPS surface sensitivity and with factors such as the density of the sample and its morphology (**Jhons & Gier**, 2001). Hence, a discussion about the structural properties is possible only if the composition of the most external layers is representative of its mass composition.

In this context, the present study assessed the composition, distribution and chemical state of the modifying species in vermiculite pillared with Al-M solutions, where M corresponds to an acidic metal (M= zirconium - Zr, cerium –Ce, and hafnium -Hf) added to the aluminum pillaring solution. X-ray diffraction (XRD), X-ray photoelectron spectroscopy (XPS), X-ray fluorescence (XRF), inductive plasma spectrometry emission (ICPS) and adsorption of nitrogen were used as characterization techniques.

Experimental process

Materials

The starting vermiculite (labeled V) corresponded to a clay mineral with a high laminar charge from the Santa Marta region in Colombia:

$$[(Si_{3.04}Al_{0.92}Ti_{0.04})(Al_{0.11}Fe^{3+}_{0.35}Fe^{2+}_{0.07}Mg_{2.41}Mn_{0.003})O_{10}(OH)_2]Ca_{0.21}K_{0.05}Na_{0.10}$$

Modifications were made to the fraction with a particle size less than 150 μm, which was separated from the raw vermiculite through sieving, with no prior purification, and had a cationic exchange capacity of 1.10 meq g^{-1} (**Campos, *et al.***, 2009).

Charge reduction treatment

Natural vermiculite was submitted to hydrothermal treatment, aiming its charge reduction at 400 °C under a partial water vapor pressure of 75% in nitrogen, according to conditions established previously (**Cristiano, *et al.***, 2005). This solid was used as a starting material in the synthesis and labeled as H400V75.

With the purpose of achieving more efficiency during the process of inserting the pillaring species within the clay layers, H400V75 was then homoionized with sodium by adding a 3 M sodium chloride solution to a suspension of the solid at 5% p/v under constant magnetic stirring for one hour at 80ºC. Finally, the clays were washed with distilled water and dried in air at 60°C.

Modification with Al-Zr, Al-Hf and Al-Ce

The polymeric solutions of Al-M (where M=Zr, Hf or Ce) were prepared to supply 12 mmol of Al+M per gram of clay (**del Rey-Pérez-Caballero & Poncelet**, 2000a). A 0.1 M solution of M was slowly added to a 0.1 M solution of $AlCl_3$ (Aldrich, anhydrous, powder, 99.999%) for the addition of Zr or Hf, or $Al(NO_3)_3$ (Aldrich, ACS reagent, ≥98%) for the addition of Ce, starting from aqueous solutions of $ZrOCl_2$

(Sigma-Aldrich reagent grade, 98%), $HfCl_4$ (Aldrich, 98%) or $Ce(NO_3)_3$ (Aldrich, 99.99% trace metals basis), respectively, under constant magnetic stirring at room temperature.

When the temperature of the Al-M solution increased to 60ºC, a 0.2 M solution of NaOH (Sigmma-Aldrich ≥98% pellets (anhydrous)) was added in a drip under vigorous stirring using the necessary volume to attain a molar ratio OH/(Al+M) of 2. At the end of the addition, the solution remained at the same temperature for 2 h. The pH of the solutions was 3.5-4.

After aging the pillaring solution for 36 h at room temperature, we slowly added it to a clay suspension (2% wt) with constant stirring. During the exchange the temperature was 80ºC, preserved for an additional 4 h after the end of the addition. The final clay suspension was aged for 12 h at room temperature. Afterward, excess salt was removed by rinsing with distilled water. Finally, the materials were dried at 60°C and calcinated at 400°C (5°C min^{-1}) for 2 h in air.

The metal ratios were selected according to the optimal value of 12 mmol of metal/g of clay for the pillaring of vermiculite through aluminum (**del Rey-Pérez-Caballero & Poncelet**, 2000a) making sure that the concentration of the second metal was not too high to prevent changes in the optimal conditions for the formation of the Al polymer (**Bottero, *et al.***, 1980).

The materials were labeled with the name of the second metal added to the aluminum polymeric solution, followed by the amount added (0.5, 1, 1.5, 2 and 4 mmol). Thus, Zr0.5 corresponds to vermiculite modified with an Al-Zr solution containing 11.5 mmol of Al and 0.5 mmol of Zr per gram of clay.

Characterization

X-ray diffraction (XRD) spectra of powder samples was measured on a Phillips PW1710 spectrometer with copper anticathode. Nitrogen adsorption isotherms were taken at 77K in a Micrometrics Tristar 3000 instrument on samples previously outgassed at 200ºC for 6 h.

XPS analyses were performed on a Kratos Axis Ultra spectrometer (Kratos Analytical – Manchester – UK) equipped with a monochromatized aluminum X-ray source (powered at 10 mA and 15 kV) and an eight channeltrons detector. The sample powders were pressed into small stainless steel troughs mounted on a multi-specimen holder. The pressure in the analysis chamber was approximately 10^{-6} Pa. The angle (θ) between the normal to the sample surface and the direction of photoelectrons collection was approximately 0°. The pass energy of the hemispherical analyzer was set at 160 eV for the wide scan and 40 eV for narrow scans. In the latter conditions, the full width at half maximum (FWHM) of the $Ag3d_{5/2}$ peak of a standard silver sample was approximately 0.9 eV. The hybrid lens magnification mode was used with the slot aperture and the iris drive set at 0.5" resulting in an analyzed area of 700 µm x 300 µm. Charge stabilization was achieved using the manufacturer's device. The following sequence of spectra was recorded: Survey spectrum, C1s, O1s, Mg2s, Si2p, Al2p, Fe2p, C1s, and Zr3d or Hf4f or Ce3d. Finally, C1s was performed again to check for charge stability as a function of time and the absence of degradation of the sample during the analyses. The C-(C, H) component of the C1s peak of carbon was fixed to 284.8 eV to set the binding energy scale.

Molar fractions (%) were calculated using peak areas normalized on the basis of acquisition parameters after a linear background subtraction, experimental sensitivity factors (**Wagner**, 1990) and transmission function provided by the manufacturer.

Elemental analysis of both the starting mineral and Zr was performed by means of X-ray fluorescence (XRF) using the Philips FRX 2400 equipment. The Hf and Ce contents were determined by ICP spectroscopy.

Results and discussion

The XRD results, surface area (S_{BET}) and microporous volume (V_{micro}) are summarized in Table 1. In general, all solids showed a substantial change with respect to the starting vermiculite H400V75, highlighting the successful pillaring procedure.

Table 1. Characterization of pillared vermiculites and the starting vermiculite (H400V75)

Sample	$d_{(001)}$ (nm)	S_{BET} (m^2/g)	V_{Micro} (cm^3/g)
Zr 0.5	1.8	104	0.040
Zr 1	1.8	127	0.049
Zr 1.5	1.8	117	0.043
Zr 2	1.8	100	0.040
Zr 4	1.4	91	0.032
Hf 0.5	1.8	81	0.032
Hf 1	1.8	100	0.040
Hf 1.5	1.8	92	0.036
Hf 2	1.8	105	0.041
Hf 4	1.4	71	0.029
Ce 0.5	1.4-1.8	80	0.033
Ce 1	1.4-1.8	91	0.038
Ce 1.5	1.4-1.8	80	0.033
Ce 2	1.4-1.8	79	0.033
Ce 4	1.5	27	0.010
V	1.4	7	0.001
H400V75	1.4	44.6	0.016

The XRD analysis of modified clays revealed the introduction of the metal polyhydroxocation and the resulting formation of oxides or oxyhydroxides due to the cations employed in the interlayer spacing of the material. The shifting of d001 basal spacing from 1.38 nm (H400V75) to 1.78-1.82 nm confirmed the modification via pillaring.

The values of the surface area agreed with the results of the X-ray diffraction revealing an increase of the BET areas, which evidenced the successful pillaring of the clay and the consequent formation of microporous structures.

While the best characteristics corresponded to the series modified with Zr, they were less pronounced for the series modified with Ce. For example, the clay modified with 4 mmol of Ce (Ce4) presented a considerable reduction in surface area with respect to other solids of the same series, as well as a low micropore volume, thus explaining the absence of a characteristic pillar signal in the XRD.

When the addition of the second cation for the series of Al-Zr and Al-Hf amounted to 4 mmol g^{-1} of clay, a notable reduction in surface area and micropore volume were also observed, although not as marked as in the case of Ce4. Such behavior may be related to the distortion of the polymeric structure of aluminum pillars, as it has been previously observed (**Bottero, *et al.***, 1980), leading to the generation of oligomers of smaller size, and/or to the generation of aggregates that may obstruct the porosity generated during the modification.

Al-Zr vermiculites

The results of elemental characterization by means of the XPS technique in vermiculites pillared with Al-Zr solutions are shown in Table 2. The five solids assessed did not show significant variations in the binding energy (BE) of the $Zr3d_{5/2}$ peak, which indicates that the same type of exchanged Zr species was obtained independently from the metal content.

Likewise, our results suggest the existence of interactions between the metal and the mineral. To elucidate the type of species and interaction, BE variations of the clay mineral must be taken into account before (H400V75) and after its modification with Al-Zr solutions and/or the formation of species such as Zr-Ox-, Zr-Si- and/or Zr-Al. As shown in Table 2, differences in the mineral before and after its modification were not very significant except for O1s and Si2p binding energy, which was ~0.4 to 0.8 eV lower in Zr samples. The discrepancy was slightly greater with the lower content of Zr (Zr0.5). These significant differences of BE suggest changes in the chemical surroundings of O and Si from vermiculite layers caused by the insertion of the Al-Zr pillaring species. In five of the clays assessed, the $Zr3d_{5/2}$ peak of the Zr3d doublet was at 182.8 eV (Figure 1A).

Table 2. Binding energies (BE in eV) for several elements in pillared vermiculites and starting material (H400V75)

Sample	O 1s	Si 2p	Al 2p	Fe $2p_{3/2}$	Mg 2s	M[a]
H400V75	532.3	103.1	74.5	712.5	89.3	
Zr 0.5	531.5	102.3	74.5	712.1	88.8	182.7
Zr 1	531.8	102.7	74.6	712.2	89.0	182.8
Zr 1.5	531.9	102.6	74.7	711.9	89.1	182.8
Zr 2	531.6	102.6	74.5	712.4	88.8	182.8
Zr 4	531.6	102.5	74.4	712.0	88.9	182.8
Hf0.5	531.7	102.6	74.6	711.6	88.6	17.5
Hf1	531.8	102.5	74.8	712.0	88.9	17.5
Hf1.5	531.6	102.6	74.6	711.6	89.0	17.4
Hf2	531.8	102.7	74.6	712.2	88.9	17.5
Hf4	531.5	102.6	74.4	711.7	89.0	17.5
Ce0.5	531.9	102.7	74.8	712.2	88.9	bdl
Ce1	531.8	102.5	74.6	712.1	88.9	bdl
Ce1.5	531.8	102.8	74.7	712.4	88.7	bdl
Ce2	531.8	102.5	74.6	712.2	88.8	bdl
Ce4	531.7	102.5	74.2	711.8	89.0	886.3

[a] M= Zr $3d_{5/2}$, Hf $4f_{7/2}$ or Ce $3d_{5/2}$
bdl: Below detection limit

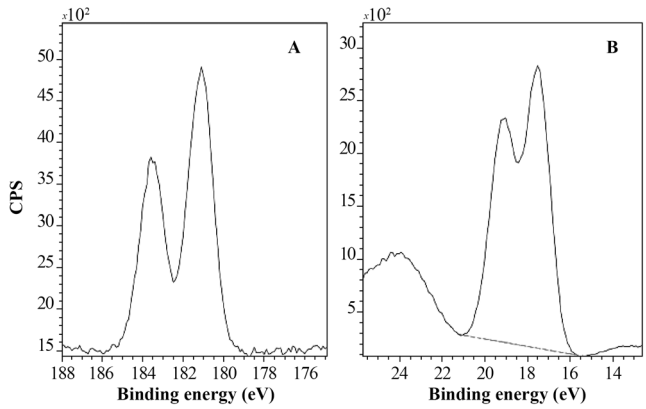

Figure 1. XPS (A) Zr-3d and (B) Hf-4f doublets recorded for vermiculite modified with Al-Zr and Al-Hf solutions

As regards the $AlZrO_x$-type materials, binding energies of 182.6 eV and 182.7-183.1 eV have been reported for the $Zr3d_{5/2}$ signal (**Damyanova, *et al.***, 2003). However, such values should be supported by variations in the Al2p BE in modified vermiculites as compared to H400V75, which were not observed in this case. The 0.8 eV difference in the binding energy of the Zr found in the modified vermiculite compared with pure ZrO_2 (182.0 eV) (**Awate, *et al.***, 2004) should be related to the formation of Zr(IV) species bound to more electron attractive species, which brings about a larger binding energy shift (**Younes, *et al.***, 2003).

Among the different possibilities, one is the presence of hydrogen associated with oxygen, as has been reported for Zr pillared montmorillonites, in which the formation of Zr-associated OH groups was suggested, with a binding energy of 182.8 eV for $Zr3d_{5/2}$ (**Awate, *et al.***, 2004). Another possibility is the presence of silicon, as the BE value for Zr (182.8 eV) was similar to the one reported for zirconium oxides supported on silica (**Fuentes, *et al.***, 2006), which indicates that the interaction of Zr on the silica surface may induce a shift in the binding energy of up to 182.9 eV.

In contrast, an increase in Al and Zr concentrations after the modifications made to the vermiculite was evident (Table 3). The introduction of aluminum in the vermiculites clearly induced a drastic reduction of the Si/Al ratio (between 1.7 and 2.1) compared to that observed in H400V75 (3.9) (Table 3).

Zr content as indicated by XPS and XRF (Table 3) did not exhibit a linear tendency with respect to the amount added to the pillaring solution. However, the introduction of a second metal to the pillared solid may be considered complete within the range of 0.5 - 2 mmol g^{-1} of clay, while with larger quantities (4 mmol g^{-1} of clay) the efficiency in the insertion, as calculated from the XRF-measured Zr and the Zr added to the pillaring solution, dropped to 69% (Table 3).

Table 3. Surface XPS values (molar fractions in %) and metal content for pillared vermiculites

Sample	M[a] (%) XPS	M (%) Bulk[b]	Ratio XPS/Bulk	Ratio Si/Al[c]	Ratio M/Si[d]
H400V75	-	-	-	3.9	-
Zr 0.5	1.6	0.19	8.3	1.7	0.1
Zr 1	2.2	0.25	8.9	1.8	0.2
Zr 1.5	1.9	0.20	9.5	2.0	0.1
Zr 2	2.7	0.23	11.8	2.0	0.2
Zr 4	2.2	0.25	8.8	2.1	0.1
Hf 0.5	1.2	0.20	5.8	2.2	0.1
Hf 1	1.4	0.24	5.8	2.3	0.1
Hf 1.5	2.8	0.39	7.2	2.0	0.2
Hf 2	1.7	0.35	4.9	2.1	0.1
Hf 4	1.5	0.33	4.6	2.2	0.1
Ce 0.5	bdl	0.12	-	1,8	-
Ce 1	bdl	0.16	-	2.0	-
Ce 1.5	bdl	0.27	-	2.1	-
Ce 2	bdl	0.29	-	1.9	-
Ce 4	0.75	0.56	1.3	2.3	0.02

[a] M= Zr, Hf or Ce
bdl: Below detection limit
[b] Total metal content: Zr by XRF, Hf and Ce by ICPS
[c, d] Element ratio (XPS)
( ) = % Efficiency on metal adding on vermiculite = % M assessed / %M in solution x 100

In the five synthesized solids, the relative Zr concentrations measured by XPS were markedly higher than those measured by XRF (Table 3), which could be explained by the preferential location of Zr outside the clay layers.

Al-Hf vermiculites

The five solids did not show any significant variation in the binding energy of the $Hf4f_{7/2}$ peak (Table 2), indicating that the same type of Hf species is found in the clay, independently of the metal content. The most significant differences between the mineral before and after modification were registered in O1s BE, and in Si2p peaks. A small shift of 0.3 to 0.9 eV was observed in the $Fe2p_{3/2}$ peak of the modified clays: 0.5 to 0.6 eV for the O1s peak and 0.5 to 0.6 eV for the Si2p peak. Consequently, a change in the chemical surroundings of these elements caused by the insertion of species of the Al-Hf pillaring solution may have occurred.

The $Hf4f_{7/2}$ peak (Figure 1B), at approximately 17.5 eV, was attributed to interactions of Hf with elements other than oxygen; for the HfO_2, the Hf $4f_{7/2}$ peak is located at approximately 16.8 eV (**Yakamoto, *et al.***, 2002). The formation of HfSiO- was discarded because this would have caused a shift of the $Hf4f_{7/2}$ peak to a binding energy of more than 1 eV as compared with that of HfO_2 (**Renault, *et al.***, 2003; **Deshpande, *et al.***, 2006). In contrast, the formation of HfAlO- species cannot be discarded because the corresponding $Hf4f_{7/2}$ peak has also been reported to be approximately 17.5 eV (**Lee, *et al.***, 2003).

Al introduction in Hf-vermiculites is clearly indicated by the drastic reduction of the Si/Al ratio (between 2.0-2.3, Table 3) compared to H400V75 (3.9 in Table 3).

Regarding the quantities of Hf used in the synthesis, the introduction of this element was complete in the range between 0.5 and 2 mmol g^{-1} of clay, but in larger quantities (4 mmol) the efficiency of the introduction was reduced to 45% compared with the initial nominal quantity. Although there was no linear tendency with respect to the Hf added and the one found in the solids, a linear increase was clearly identified in catalysts Hf0.5 to Hf1.5, while for catalysts Hf2 and Hf4 the metal content was reduced in the bulk (Table 3).

Hf content was larger on the surface (XPS) than in the bulk (ICPS), an the same was observed for Zr (Table 3), which suggests the preferential presence of these elements outside the clay layers.

Al-Ce vermiculites

As shown in Table 2, the most significant difference between the starting mineral and the clays after modification concerned

the BE of the O1s, Si2p and Mg2s peaks. In modified clays those peaks were shifted to a lower BE than that of the respective peak in H400V75: between 0.4 and 0.6 eV for the O1s signal; between 0.3 and 0.6 eV for the Si2p signal, and between 0.3 and 0.6 eV for the Mg2s signal. These shifts suggested an eventual effect of cerium on the mineral surface, but Ce was detectable only in the Ce4 sample and not in the other samples. The Ce3d doublet overlapped with the $FeL_2M_{2,3}L_{2,3}$ Auger peak, which was situated between the two peaks of the Ce3d doublet (Figure 2). The Ce4 sample had the lowest iron concentration, which explains why the Ce3d doublet, although overlapped with Fe Auger, could be detected. However, the measured concentration of Ce may have been overestimated due to the presence of this Fe Auger peak. Consequently, compared to the two other metals Ce cannot be quantified reliably from the Ce3d peak despite its high cross section (**Scofield**, 1976).

The characteristic feature of the Ce3d spectrum of Ce^{4+} is the existence of a high BE satellite at ~916 eV (**Mamede, *et al.***, 2004; **Hashimoto, *et al.***, 1997), which is absent from the Ce3d spectrum of Ce^{3+} (**Hashimoto, *et al.***, 1997). In our case, the satellite was absent from the Ce3d spectrum recorded for Ce4 (Figure 2), and, therefore, there was only Ce^{3+} and no Ce^{4+}.

Regarding the total bulk concentration of Ce registered in the ICPS (Table 3), a linear tendency was observed with respect to the nominal quantity used in the synthesis within the evaluated range. Given that the ICPS quantification of Ce demonstrated its incorporation into the five modified

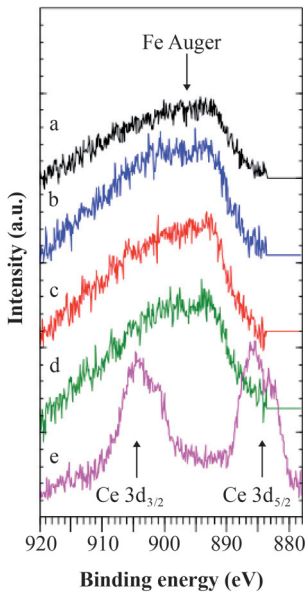

Figure 2. XPS Ce3d doublet recorded for vermiculite modified with Al-Ce solutions: (a) Ce0.5, (b) Ce1, (c) Ce1.5, (d) Ce2, (e) Ce4

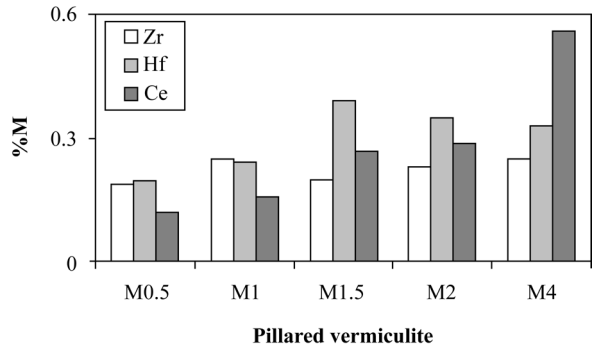

Figure 3. Total metal content (M=Zr, Hf or Ce) assessed for pillared vermiculites with Al-Zr (Zr), Al-Hf (Hf) and Al-Ce (Ce) solutions

solids (Figure 3), and that it could not be detected by XPS, it may have been located inside the clay aggregates in solids Ce0.5 to Ce2. Additionally, in Ce4, the Ce/Si ratio (0.02) was very low compared to that in Zr4 and Hf4 (0.15 and 0.11, respectively), although Ce content in bulk was larger, which indicates that Ce was present in the aluminum polymer solution, but its interaction with the clay during the modification process was different from that of Zr and Hf.

Such behavior of Ce in the vermiculites is similar to the one previously reported in pillared montorillonites modified with mixed Ce-Zr (**Mishra & Rao**, 2003) and Ce-Al species (**Mishra & Rao**, 2005), in which it has been proposed that starting from the UV-VIS diffuse reflectance analysis, the Ce^{3+} ions were located preferentially in the exchange sites of clays or that they were associated to the pillaring generated micropores.

In contrast, our results showed that Zr and Hf most likely precipitated as oxides on the outer surface of clay particles because these ions precipitate at pH=1 while Ce^{3+} species exist up to a pH=7 level (**Jolivet, *et al.***, 1994).

Conclusions

The total content of the metals added to the aluminum solution for the pillaring process showed that the introduction of Ce was complete in the range of 0.5 - 4 mmol g^{-1} of clay, whereas for Hf and Zr, it was in the range of 0.5-2 mmol g^{-1} of clay.

The peak binding energies of $Zr3d_{5/2}$, $Hf4f_{7/2}$, $Ce3d_{5/2}$ indicated that these metals were found as Zr^{4+}, Hf^{4+} and Ce^{3+}, respectively.

The low XPS signal observed in the Ce4-vermiculite and the absence of the 3d signals in other clays modified with Ce indicate that probably Ce is preferentially located in the internal regions of clay aggregates. In contrast, our results showed that Zr and Hf were preferentially located at the outer surface of clay particles.

Bibliography

Awate S., Waghmode S., Agashe M. (2004). Synthesis, characterization and catalytic valuation of zirconia-pillared montmorillonite for linear alkylation of benzene. Catal. Commun. **5**: 407-411.

Bottero J., Cases J., Flessinger F., Poirier J. (1980). Studies of hydrolyzed aluminum chloride solutions. Nature of aluminum species and composition of aqueous solutions. J. Phys. Chem. **84**: 2933-2939.

Campos A., Gagea B., Moreno S., Jacobs P., Molina R. (2007). Hydroisomerization of decane on Pt/Al,Ce-pillared vermiculites. Stud. Surf. Sci. Catal. **170**: 1405-1409.

Campos A., Moreno S., Molina R. (2008a). Relationship between hydrothermal treatment parameters as a strategy to reduce layer charge in vermiculite, and its catalytic behavior. Catal. Today. **133-135**: 351-356.

Campos A., Gagea B., Moreno S., Jacobs P., Molina R. (2008b). Decane hydroconversion with Al-Zr, Al-Hf, Al-Ce-pillared vermiculites. Appl. Catal. A. **345**: 112-118.

Campos A., Moreno S., Molina R. (2009). Characterization of vermiculite by XRD and spectroscopic techniques. Earth Sci. Res. J. **13**: 108-118.

Chmielarz L., Kus´trowski P., Michalik M., Dudek B., Piwowarska Z., Dziembaj R. (2007). Vermiculites intercalated with Al_2O_3 pillars and modified with transition metals as catalysts of DeNOx process. Catal. Today. **137**: 242-246.

Cool P., Clearfield A., Mariagnanam V., Ellistrem L., Crooks R., Vansant E. (1997). Self-assembly of aluminium-pillared clay on a gold support. J. Mater. Chem. **7**: 443-448.

Cristiano D., Campos A., Molina R. (2005). Charge reduction in a vermiculite by acid and hydrothermal methods: A comparative study. J. Phys. Chem B. **109**: 19026-19033.

Damyanova S., Petrov L., Grange P. (2003). XPS characterization of zirconium-promoted CoMo hydrodesulfurization catalysts. Appl. Catal. A. **239**: 241-252.

Deshpande A., Inman R., Jursich G., Takoudis C. (2006). Characterization of hafnium oxide grown on silicon by atomic layer deposition: Interface structure. Microelectron. Eng. **83**: 547-552.

Fuentes D., Santamaría J., Mérida J., Rodríguez F., Jiménez A., Maireles P., Moreno R., Mariscal R. (2006). Evaluation of the acid properties of porous zirconium-doped and undoped silica materials. J. Solid State Chem. **179**: 2182-2189.

González A., Espinòs J., Munuera G., Sanz J., Serratosa J. (1988). Bonding-state characterization of constituent elements in phyllosilicate minerals by XPS and NMR. J. Phys. Chem. **92**: 3471-3476.

Hernández W., Moreno S., Molina R. (2007). Modificación y caracterización de una vermiculita colombiana con especies de titanio, zirconio y sulfato. Rev. Col. Quím. **36**: 73-91.

Hernández W., Centeno M., Odriozola J., Moreno S., Molina R. (2008). Acidity characterization of a titanium and sulfate modified vermiculite. Mater. Res. Bull. **43**: 1630-1640.

Jhons W. & Gier S. (2001). X-ray photoelectron spectroscopic study of layer charge magnitude in micas and illite-smectite clays. Clay Miner. **36**: 355-367.

Jiménez M., Pérez-Rodríguez J., Poyato J., Pérez-Maqueda L., Ramírez V., Justo A., Lerf A., Wagner F. (2005). Effect of ultrasound on preparation of porous materials from vermiculite. Appl. Clay Sci. **30**: 11-20.

Jolivet J., Henry M., Livage J. (1994). De la solution á l'oxyde. Intermédiations, Paris, p. 68.

Gier S. & Johns W. (2000). Heavy metal-adsorption on micas and clay minerals studied by X-ray photoelectron spectroscopy. Appl. Clay Sci. **16**: 289-299.

Hashimoto K., Matzuo K., Kominami H., Kera Y. (1997). Cerium oxides incorporated into zeolite cavities and their reactivity. J. Chem. Soc., Faraday Trans. **93**: 3729-3732.

He H., Zhou Q., Frost R., Wood B., Duong L., Kloprogge J. (2007). A X-ray spectroscopy study of HDTMAB distribution within organoclays. Spectrochim. Acta, Part A. **66**: 1180-1188.

Lee P., Dai J., Wong K., Chan H., Choy C. (2003). Growth and characterization of Hf-aluminate high-*k* gate dielectric ultrathin films with equivalent oxide thickness less than 10 Å. J. Appl. Phys. **93**: 3665-3667.

Mamede A., Payen E., Grange P., Poncelet G., Ion A., Alifanti M., Pârvulescu V. (2004). Characterization of WOx/CeO_2 catalysts and their reactivity in the isomerization of hexane J. Catal. **223**: 1-12.

Mishra B. & Rao G. (2003). Influence of synthesis conditions and cerium incorporation on the properties of Zr-pillared clays. J. Porous Mater. **10**: 93-103.

Mishra B. & Rao G. (2005). Cerium containing Al- and Zr-pillared clays: Promoting effect of cerium (III) ions on structural and catalytic properties. J. Porous Mater. **12**: 171-181.

Pandolfi L., Cafarelli P., Kasiulis S., Tomlinson A. (2008). XPS analysis of several zeolites and clay-based nanoporous materials for C4 hydrocarbon conversions. Microporous Mesoporous Mater. **110**: 64-71.

Purceno A., Teixeira A., Souza A., Ardisson J., Mesquita J., Lago R. (2012). Ground vermiculite for the Fenton reaction. Appl.Clay Sci. **69**: 87-92.

Renault O., Samour D., Rouchon D., Holliger P., Papon A., Blind D., Marthon S. (2003). Interface properties of ultra-thin HfO_2 films grown by atomic layer deposition on SiO_2/Si Thin Solid Films. **428**: 190-194.

del Rey-Pérez-Caballero F. & Poncelet G. (2000a). Microporous 18 Å Al-pillared vermiculites: Preparation and characterization. Microporous Mesoporous Mater. **37**: 313-327.

del Rey-Pérez-Caballero F. & Poncelet G. (2000b). Preparation and characterization of microporous 18 Å Al-pillared structures from natural phlogopite micas. Microp. Mesop. Mater. **41**: 169-181.

del Rey-Pérez-Caballero F., Sánchez M., Poncelet G. (2000c). Hydroisomerization of octane on Pt/Al-pillared vermiculite, and comparison with zeolites. Stud. Surf. Sci. Catal. **130**: 2417-2422.

Scofield J. (1976). Hartree-Slater subshell photoionization cross-sections at 1254 and 1487 eV. J. Electron Spectrosc. Relat. Phenom. **8**: 129-137.

Suvorov D. & Skurikhin V. (2003). Vermiculite: A promising material for high-temperature heat insulators. Refract. Ind. Ceram. **44**: 186-193.

Tanabe K., Misono M., Ono Y., Hattori H. (1989). New Solids Acids and Bases: Their Catalytic Properties. Stud. Surf. Sci. Catal., Elsevier, Amsterdam, **51**: 108.

Trombetta M., Lenarda M., Storaro L., Gonzerla R., Piovesan L., Jiménez A., Alcántara M., Rodríguez E. (2000). Solid acid catalysts from clays: Evaluation of surface acidity of mono- and bi-pillared smectites by FT-IR spectroscopy measurements, NH_3-TPD and catalytic tests. Appl. Catal. A. **193**: 55-69.

Valášková, M., Tokarský, J., Hundáková, M., Zdrálková, J., Smetana, B. (2013). Role of vermiculite and zirconium–vermiculite on the formation of zircon–cordierite nano-composites. Appl. Clay Sci. **75–76**: 100-108.

Vicente, M. A., Gil, A., Bergaya, F. (2013). Chapter 10.5 - Pillared Clays and Clay Minerals. Developments in Clay Science. B. Faïza and L. Gerhard (¿editors?) Elsevier. **5**: 523-557.

Wagner C. (1990). Practical Surface Analysis. Second ediction. J. Wiley and Sons (Eds). (¿Ciudad? ¿Páginas?).

Weckhuysen B., Van Der Voort P., Catana G. (2000). Spectroscopy of Transition Metal Ions on Surfaces. Leuven University Press. Belgium.

Yakamoto K., Hayashi S., Kubota M., Niwa M. (2002). Effect of Hf metal predeposition on the properties of sputtered HfO_2/Hf stacked gate dielectrics Appl. Phys. Lett. **81**: 2053-2056.

Younes M., Ghorbel A., Rives A., Hubaut R. (2003). Comparative study of the acidity of sulphated zirconia supported on alumina prepared by sol-gel and impregnation methods. J.Sol-Gel Sci. Technol. **26**: 677-680.